Chemistry and Physics of Lipids 263 (2024) 105418

Contents lists available at ScienceDirect

Chemistry and Physics of Lipids

journal homepage: www.elsevier.com/locate/chemphyslip

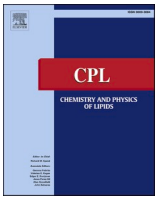

Structural characterization of cholesterol-rich nanoemulsion (LDE)

Aline S. Perez [a], Aleksandra T. Morikawa [b], Raul C. Maranhão [b], Antônio M. Figueiredo Neto [a,b,*]

[a] Institute of Physics, University of São Paulo, Rua do Matão 1371 - Butantã, São Paulo, SP 05508-090, Brazil
[b] Lipid Metabolism Laboratory, Heart Institute of the Medical School Hospital (InCor), University of São Paulo, Av. Dr. Enéas Carvalho de Aguiar, 44 - Cerqueira César, São Paulo, SP 05403-900, Brazil

ARTICLE INFO

Keywords:
Nanoparticle structure
Emulsions
Solid lipid particles
Etoposide
Paclitaxel
Methotrexate
SAXS
DLS

ABSTRACT

Cholesterol-rich nanoemulsion (LDE) can carry chemotherapeutic agents in the circulation and can concentrate those agents in the neoplastic and inflammatory tissues. This method improves the biodistribution of the drug and reduces toxicity. However, the structural stability of LDE particles, without or with associated drugs, has not been extensively investigated. The aim of the present study is to investigate the structural stability of LDE and LDE associated to paclitaxel, etoposide or methotrexate in aqueous solution over time by small-angle X-ray scattering (SAXS and Ultra SAXS) and dynamic light scattering (DLS). The results show that LDE and LDE associated with those chemotherapeutic agents had reproducible and stable particle diameter, physical structure, and aggregation behavior over 3-month observation period. As estimated from both DLS and Ultra-SAXS methods, performed at pre-established intervals, the average particle diameter of LDE alone was approx. 32 nm, of LDE-paclitaxel was 31 nm, of LDE-methotrexate was 35 nm and of LDE-etoposide was 36 nm. Ultra-SAXS analysis showed that LDE nanoparticles were quasi-spherical, and SAXS showed that drug molecules inside the particles showed a layered-like organization. Formulations of LDE with associated PTX, ETO or MTX were successfully tested in animal experiments and in patients with cancer or with cardiovascular disease, showing markedly low toxicity, good tolerability and possible superior pharmacological action. Our results may be useful for ensuing clinical trials of this novel Nanomedicine tool, by strengthening the knowledge of the structural aspects of those LDE formulations.

1. Introduction

Cancer chemotherapy is usually performed with the combination of two or more antineoplastic drugs. Combined chemotherapy can affect the metabolic pathways of cancer cells by different mechanisms. This improves the pharmacological effect and may reduce the development of drug resistance in cancer cells. However, treatment with combined chemotherapy can increase the toxicities of the therapy. A possible strategy to reduce the toxicity of chemotherapeutic agents is to incorporate drugs into delivery systems, such as liposomes or other nanoparticles that could specifically target neoplastic tissues.

A cholesterol-rich nanoemulsion (LDE) has been used as a vehicle to target antineoplastic drugs against cancer cells, as shown by the pioneer studies by (Maranhão et al., 1994). LDE resembles the structure of Low-Density Lipoprotein (LDL), but lacks apolipoprotein (apo) B, the single protein in LDL (Maranhão et al., 1994). The nanoemulsion composition allows LDE to acquire apo E from the native lipoproteins, which endows the nanoemulsion with the ability of being recognized by LDL receptors (Fig. 1).

Apo E bridges LDE for cell internalization via LDL receptor mediated endocytosis (Maranhão et al., 1993). Since cancer cells show upregulation of LDL receptors, LDE can be used as a vehicle to direct antineoplastic drugs to those cells. The association of antineoplastic drugs, as methotrexate (MTX), paclitaxel (PTX), and etoposide (ETO) to LDE is stable and retains the cytotoxic activity of those drugs. As LDE is artificially-made it is important that the size of the particles be as close as possible to LDL the native apo, to allow receptor binding. This highlights the importance of characterization that show the size distribution and structural stability of LDE-drug formulations. The association to LDE of chemotherapeutic agents such as MTX, PTX and ETO results in pronounced reduction of toxicity as shown in mice and rats essays (Teixeira et al., 2010; Valduga et al., 2010; Prete et al., 2010). The

* Corresponding author at: Institute of Physics, University of Sao Paulo, Rua do Matão, 1371 - Butantã, São Paulo, SP 05508-090, Brazil.
E-mail address: afigueiredo@if.usp.br (A.M. Figueiredo Neto).

https://doi.org/10.1016/j.chemphyslip.2024.105418
Received 27 March 2024; Received in revised form 22 May 2024; Accepted 26 June 2024
Available online 27 June 2024

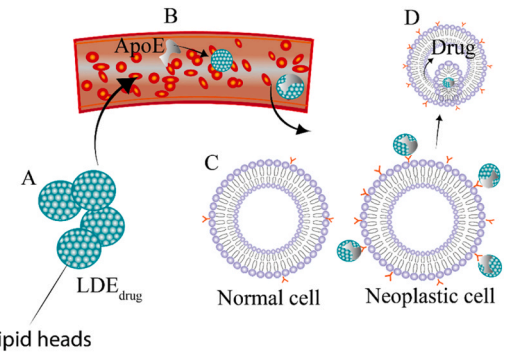

Fig. 1. A) Low density emulsion – LDE-associations are inserted into the patient bloodstream, where B) LDE-drug particles can incorporate apo E. C) normal cells have a regulated number of LDL receptors differently neoplastic cells which have an increased number, of receptors, due the high demand for cholesterol and lipids for cell duplication. D) as LDE has great affinity for the receptors, the nanoparticle is incorporated into the cell and the drug is released.

reduction of the toxicity of ETO and PTX was also shown in clinical assays enrolling patients with advanced stages of cancers (Pinheiro et al., 2006; Dias et al., 2007).

Lipid nanoemulsions are colloidal systems with a core-shell structure, featuring lipids as the major components (Greenwood et al., 2006). The small droplet size of nanoemulsions, typically in the nanometer range, enhances their stability and biocompatibility (Schneider et al., 1973). Structural characteristics of LDE can impact binding to LDL receptors. The size of nanoemulsion droplets plays a crucial role in determining their circulation time and biodistribution. Nanoemulsion size can be tailored for specific therapeutic applications, optimizing drug delivery efficiency. The composition of lipid nanoemulsions can affect recognition by specific cell receptors.

Size and form modifications of nanoemulsions can further modulate their receptor binding properties (Priya et al., 2022). Ligand-functionalized of those structures can enhance their specificity to target receptors, promoting targeted drug delivery. Size-dependent interactions are critical in regulating the cellular internalization kinetics of nanoemulsions (Mahato, 2017). The ability to investigate the nanoparticles size provides a versatile platform for personalized medicine. Structural characteristics, as size, surface area and polydispersity in solution can influence the pharmacokinetics of nanoemulsion-based drug delivery systems. The particles can be engineered to avoid recognition by the reticuloendothelial system, prolonging circulation time. The design of lipid-rich particles considers factors such as particle size, surface charge, and ligand conjugation. The size-dependent interactions with receptors are essential for achieving site-specific drug delivery and minimizing off-target effects (Ahmed and Dash, 2017).

In this work, we investigate the structure of LDE and LDE-associated particles using (Ultra) Small Angle X-ray Scattering (SAXS) technique and Dynamic Light Scattering (DLS). The discussion of the results and analysis of the structural properties of the particles are compared to DLS measurements done in previous studies (Prete et al., 2010; Pires et al., 2009; Maranhao et al., 2011).

2. Material and methods

2.1. LDE preparation

LDE was synthesized from a lipid mixture composed of 40 mg cholesteryl oleate, 20 mg egg phosphotidylcholine, 1 mg triolein and 0.5 mg cholesterol (all lipids were purchased from Nu-Check Prep, Elysian, MN). [^{14}C] cholesteryl ester was added to the mixture (purchased from Amersham International, Amersham, UK). The emulsification of lipids by prolonged ultrasonic irradiation in aqueous media and the two-step ultracentrifugation procedure of the crude emulsion with density adjustment by addition of KBr to obtain LDE microemulsion was carried out by the method modified by (Maranhão et al., 1993). LDE was dialyzed against saline solution and passed through 0.22 μm filter (Millipore, Billerica, MA, USA).

2.2. Preparation of LDE and association with methotrexate (LDE-MTX)

LDE-MTX was prepared from a lipid mixture composed of 100 mg cholesteryl oleate, 200 mg egg phosphatidylcholine (Merck, Hohenbrum, Germany), 10 mg triglycerides, 12 mg cholesterol and 60 mg of MTX (R. Maranhão et al., 2011; R. C. Maranhão et al., 1992). The aqueous phase (100 mg of polysorbate 80 and 10 mL of Tris-HCl buffer, pH 8.05) at 25 °C. Emulsification was performed by high-pressure homogenization using an Emulsiflex C5 homogenizer (Avestin, Ottawa, Canada). After homogenization at constant temperature, the nanoemulsion was centrifuged at 1800 g for 15 min at 4°C to separate the emulsified from unbound MTX. The nanoemulsion was sterilized by passage through 0.22 μm pore filter (Millipore, Billerica, MA, USA) and kept at 4°C. The association of MTX to LDE was measured by HPLC before the treatment (Mello et al., 2013).

2.3. Preparation of LDE and association with paclitaxel (LDE-PTX)

LDE was prepared from a lipid mixture composed of 40 mg cholesteryl oleate, 20 mg egg phosphaditylcholine, 1 mg triolein and 0.5 mg cholesterol. Emulsification of lipids by prolonged ultrasonic irradiation in aqueous media. Two-step ultracentrifugation of the raw emulsion with density adjustment by addition of KBr were done to obtain LDE. The solution was sonicated for 30 min at 70°C using a Branson Sonifier 450 (Danbury, CT, USA), equipped with a 1 cm flat titanium probe. LDE–paclitaxel oleate was centrifuged at 3000 rpm for 15 min to separate the unbound paclitaxel oleate. LDE–paclitaxel oleate was then passed through a 0.22 μm pore polycarbonate filter and kept at 4°C until use (Pepineli et al., 2021).

2.4. Preparation of LDE and association with etoposide (LDE-ETO)

LDE (1 mL) was added over 6.0 mg etoposide oleate dissolved in 100 μL ethanol. In those conditions, the drug precipitated as a very slight powder and the dissolution into LDE was facilitated. The solution was sonicated for 40 min at 55 °C using a Branson Sonifier 450 (Danbury, CT, USA), with a 1 cm flat titanium probe. LDE-etoposide oleate was centrifuged (3000 g) for 45 min to separate the free etoposide oleate (pellet) from the association LDE-etoposide oleate (supernatant). The pellet was dissolved in 1 mL methanol and quantified by HPLC to give the final yield of association by diminishing the amount of free drug from the total added at the beginning of the procedure. LDE-etoposide oleate was then passed through a 0.22 μm pore polycarbonate filter and kept at 4 °C until use (Prete et al., 2010).

2.5. Dynamic light scattering (DLS)

The hydrodynamic diameter of the particles was measured using DLS (NanoBrook 90 Plus from BrookHaven Instruments Corp.) at a scattering angle of 90° and wavelength of 657 nm. The samples were diluted, 2 mg/mL, with 0.1 M Tris buffer, placed in disposable cuvettes at room temperature (25 °C). 5 measurements of 3 minutes each were carried out for each sample. Data analysis was caried out using the method Non-Negative Least Squares (NNLS). This iterative method is adopted for multimodal systems with heterogeneous particle size distribution.

In DLS the fluctuations of the scattered intensity I at a given angle θ are accounted for by the field autocorrelation function, written as a function of the scattered intensity $I(t)$ as (for details, see Supplemental Material)

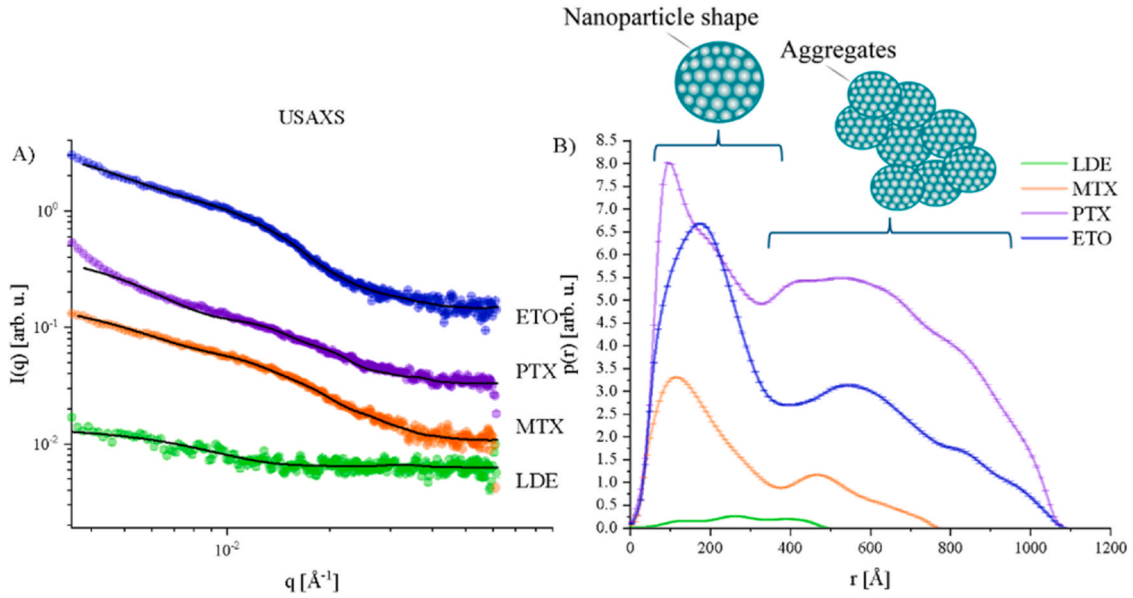

Fig. 2. USAXS experimental data (colored dots) for LDE, and LDE with drug association (PMTX: methotrexate, TX: paclitaxel and ETO: etoposide). A) Experimental data (colored circles), IFT fits (black lines). B) p(r) curves for LDE and LDE with drug association. The spheres in Fig. 2B indicate the region of single particles and aggregates.

$$g^{(1)}(\tau) = \frac{1}{\beta}\left(\frac{\langle I(t)I(t+\tau)\rangle}{\langle I(t)^2\rangle} - 1\right)^{\frac{1}{2}} \quad (1)$$

where the brackets indicate an average over time *t*, β denotes the measured value in the short-time limit (Montis et al., 2017). For a relatively polydisperse sample, the distribution of decay rates is the desired quantity: a general approach is expanding the field autocorrelation function in terms of the distribution moments of the decay rates, through the cumulant analysis, stopped at the second order, as:

$$g^{(1)}(\tau) = e^{-\Gamma_1\tau + \frac{1}{2!}\Gamma_2\tau} \quad (2)$$

with Γ_1 the intensity-weighted mean value of Γ and Γ_2 being the variance (polydispersity index, PDI) of the distribution (Koppel, 1972).

2.6. (Ultra-) small-angle X-ray scattering (USAXS/SAXS) measurements

LDE diameter in solution were also investigated by low-angle X-ray scattering (USAXS/SAXS). Measurements were carried out in buffer Tris (without dilution, [30 mg/mL]) arranged in disposable quartz capillaries, at 25 °C. The data were obtained using the Xenocs XEUSSTM equipment, with a GENIXTM source (CuKα, λ = 1.54 Å), the beam obtained is focused by FOX2D. The 2D SAXS data were collected by the Dectris PilatusTM 100k detector, which is located inside the vacuum chamber. For SAXS measurements, the sample-detector distance was 1.2 m. While for USAXS measurements the sample-detector distance was 6.5 m. In all cases, frames of 1.8×10^3 s each were obtained. The data treatment was performed using the SUPERSAXS package (Oliveira and Pedersen, unpublished) and normalized to absolute scale using water as primary standard. (U)SAXS measurements were carried out in four moments: M1 – one week after sample preparation, M2 - two weeks, M3 – six weeks and M4 - 10 weeks.

2.7. USAXS/SAXS data analysis

Several steps were performed in the SAXS data analysis. First, the data were analyzed by the indirect Fourier transformation (IFT) method (Pedersen et al., 1994). From these analyses, initial information about size, shape, and possible aggregation were obtained. For the LDE samples, it was observed that the presence of aggregates depends on the associated drug. To be able to analyze the contribution only from the LDE particles, not from the aggregates, it is necessary to decouple the form and structure factors of the scattering data. It was performed by using IFT method (GIFT) (Oliveira et al., 2009). In this case, a theoretical function is used for the structure-factor contribution, and it is possible, by simultaneous optimization of the p(r) function (form-factor) and structure-factor parameters, to obtain the theoretical form factor without the structure-factor contribution (for additional details, see the Supplemental Material). Having the form factors for each case, a complementary analysis was performed. This procedure is based on the square root deconvolution method, originally proposed by Glatter (Oliveira et al., 2009; Alanazi et al., 2015), but with a different implementation, similar to that proposed by Oliveira (Freitas et al., 2018). In this method, since the scattering data were adjusted, it is possible to introduce several types of anisotropy, e.g., as polydispersity, as well as to perform a simultaneous fitting of additional backgrounds to the scattering data and several other types of contribution (Freitas et al., 2018). The description of the normalized intensity form factor, P(q), and amplitude form factor, A(q), is performed using an analytical or semi-analytical expression written as (see Supplemental Material for details):

$$P(q) = \frac{\int_0^\infty D(r)m(r^2)P(q,r)dr}{\int_0^\infty D(r)m(r^2)dr} \quad (3)$$

$$A(q) = \frac{\int_0^\infty D(r)m(r^2)A(q,r)dr}{\int_0^\infty D(r)m(r^2)dr} \quad (4)$$

where a number distribution polydispersity in size was assumed. The function m(r) depends on the assumed geometry for the particle. For spheroidal particles, $m(r) = V$, where V is the particle volume. Different geometries may have different weighting functions.

3. Results and discussion

3.1. USAXS

Experimental data for USAXS of the LDE (green), LDE-methotrexate (orange), LDE-paclitaxel (purple), and LDE etoposide (blue) samples are

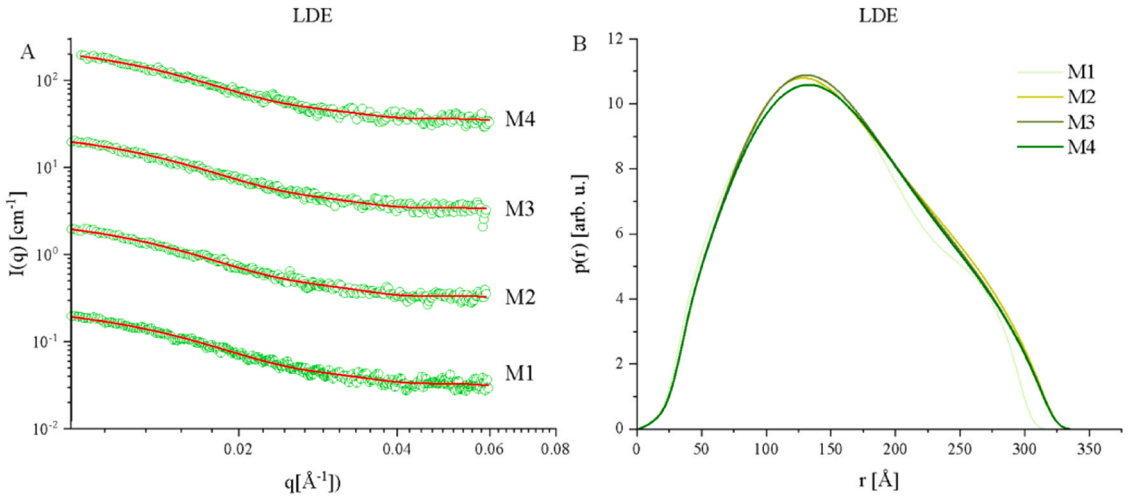

Fig. 3. Indirect Fourier Transformation (IFT) analysis applied to LDE USAXS data. A) Fitting (red curve) of scattering data (green circles) of LDE samples by the IFT method. B) Pair distance distribution functions, p(r), obtained from the decoupling procedure with IFT method for LDE samples over the time.

presented in Fig. 2. The experiments were carried out over 3 months to compare structural stability over time. Data in Fig. 2 represents the average of these experiments.

Fig. 2B shows the p(r) function, obtained from the scattering data shown in Fig. 2A. It represents the histogram of distances between pairs of points within the particle. From the analysis of Fig. 2B it is possible observe, in all the cases, the presence of aggregates in the solutions at 25 °C. This may occur due to the high concentration of nanoparticles (30 mg/mL) in the solution. Except for LDE alone, which presents a small fraction of aggregates under these conditions, with a maximum size of 50 nm, the others show the presence of aggregates. As the maximum diameter of the LDE, obtained by decoupling, is approximately 31 nm, there is a small contribution from aggregated LDE in the p(r) function. From the normalization of p(r) by the incident intensity, presented in Fig. 2S (Supplementary Material), the contribution of aggregates is evident. The formation of aggregates from approximately 36 nm is observed for MTX, PTX and ETO. The aggregates have a random shape, probably, of different sizes. The SAXS technique employed, with X-ray exposure time of the order of 1800 s, and the method of analysis of the p(r) function alone, could not give a detailed information about the actual shape of the aggregates. To obtain insights into the shape of the aggregates, we employed the *ab initio* model (DAMINN software) on the USAXS data. The shapes obtained are shown in Fig. 3S (Supplementary Material). The maximum size of the aggregates varied according to the drug associated with LDE. For LDE (~50 nm) LDE-MTX (~160 nm), LDE-PTX (~125 nm) and LDE-ETO (~165 nm).

To obtain shape information from a single LDE particle, we made the decoupling of the aggregate contribution from the individual LDE particle in the *I(q)* for each sample. With this procedure we have information about the maximum particle size and shape. The results in Fig. 3 suggest that the shape of the LDE is quasi-spherical. Previous Transmission Electron Microscopy studies also suggested that LDE particles and LDE associations are quasi-spherical in shape (Maranhao et al., 2011; Alanazi et al., 2015), which agrees with our USAXS analysis. It was possible to decouple the contribution of the aggregates, from the scattered curve results, for each sample, to obtain the form factor. Indirect Fourier transformation (IFT) method (Pedersen et al., 1994; Glatter, 1977) is used for obtaining model-independent information on the structures of the objects. The generalized IFT method provides the pair distance distribution function p(r), which gives direct information about the structure in real space. The function is a histogram of all distances between a pair of points within the particles weighted by excess electron density relative to the buffer that can be both positive

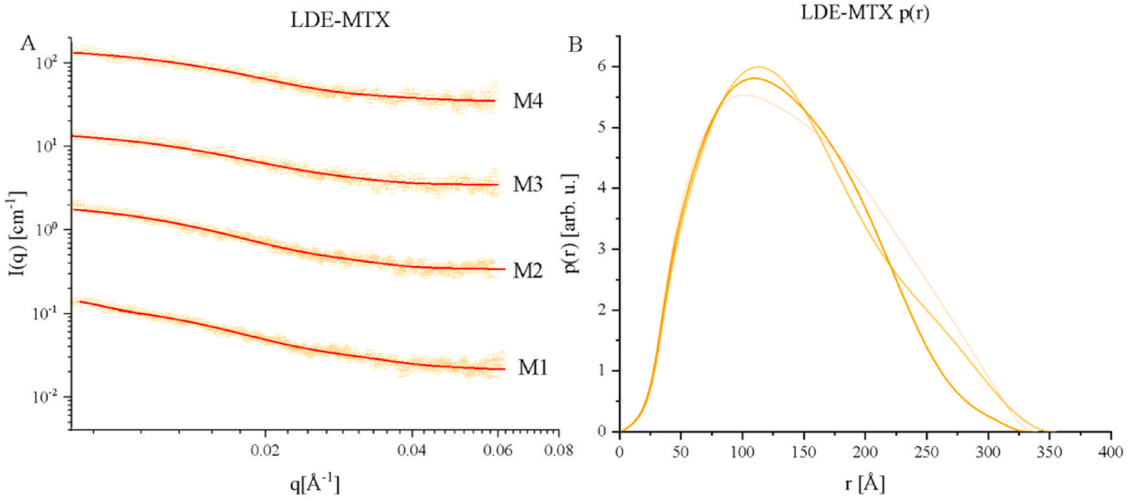

Fig. 4. IFT applied to LDE-MTX USAXS data. A) Fitting (red curve) of scattering data (orange circles) of LDE-MTX samples by the IFT method. B) Pair distance distribution functions, p(r), obtained from the decoupling procedure with IFT method for LDE-MTX samples over the time.

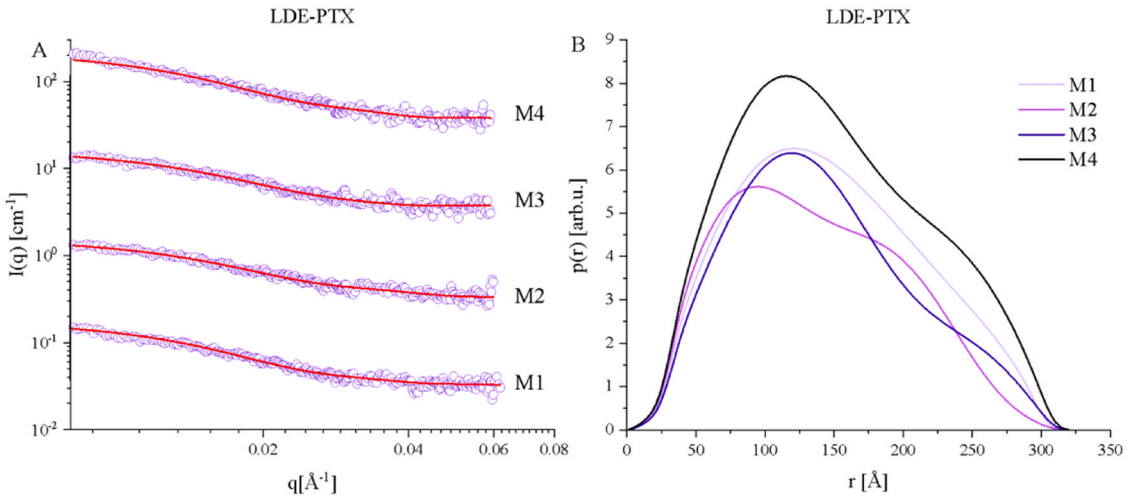

Fig. 5. IFT applied to LDE-PTX USAXS data. A) Fitting (red curve) of scattering data (purple circles) of LDE-PTX samples by the IFT method. B) Pair distance distribution functions, p(r), obtained from the decoupling procedure with IFT method for LDE-PTX samples over the time.

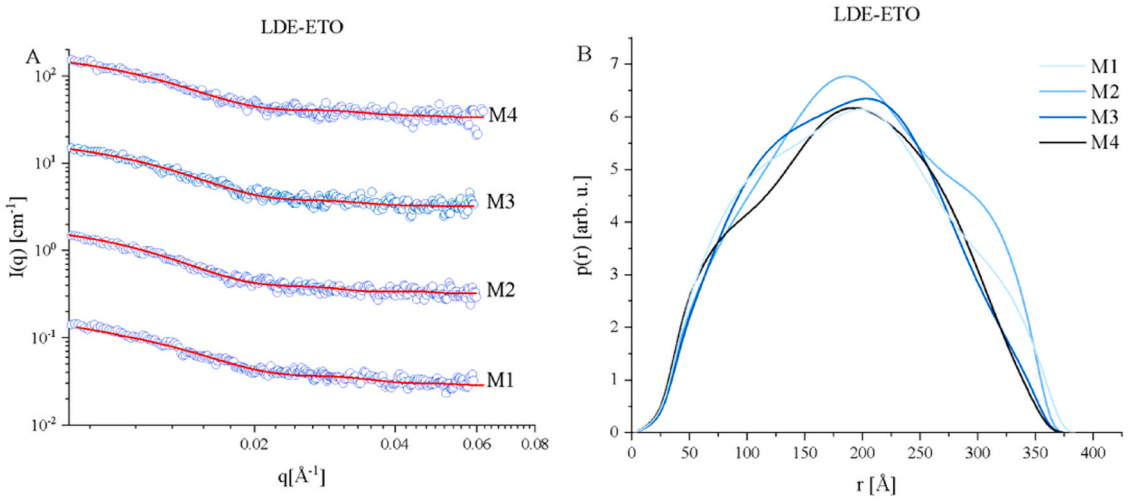

Fig. 6. IFT applied to LDE-ETO USAXS data. A) Fitting (red curve) of scattering data (purple circles) of LDE-ETO samples by the IFT method. B) Pair distance distribution functions, p(r), obtained from the decoupling procedure with IFT method for LDE-ETO samples over the time.

and negative, at each point. The function goes through zero when $r = D_{max}$, where D_{max} is the maximum distance within scattering objects. Data were obtained for LDE samples, for distinct measurements over 3 months. The results also show that the sample remains stable and presents reproducible data over the time.

Fig. 4 shows the maximum (average) diameter, of 34.5 nm, obtained for LDE-MTX samples for distinct measurements over 3 months. The results also show that the sample remains stable and presents reproducible data. Scattering results for LDE-MTX also indicate an approximately spherical shape.

Fig. 5 shows the maximum (average) diameter, of 32.0 nm, obtained for LDE-PTX samples for distinct measurements over 3 months. The results also show that the sample remains stable and presents reproducible data. Scattering results for LDE-PTX also indicate an approximately spherical shape.

Fig. 6 shows the maximum (average) diameter, of 37.5 nm, obtained for LDE-ETO samples for distinct measurements over 3 months. The results also show that the sample remains stable and presents reproducible data. Scattering results for LDE-ETO also indicate an approximately spherical shape.

As the particles are in solution, the measurements of *I(q)*, and consequently *p(r)*, are averages obtained in time and space. In such a way, these small variations in morphology (such as prolate or oblate shape factor) cannot be observed in these conditions. Therefore, more detailed studies with a different technique on possible changes in morphology are recommended in the future.

The drugs incorporated into the nanoemulsion are hydrophilic (Occhiutto et al., 2020), and therefore, are expected to be located in the hydrophilic part of the LDE (i.e., the core of the particle). Due to the mechanisms of action of LDE, it is known that the shell must be able to bind to Apo E, which in turn can bind to the LDL receptor in the cell. Therefore, the drug should not accumulate in the LDE shell. Otherwise, the drug could avoid the binding to the Apo E and, consequently, would not be internalized by the cell. Furthermore, LDE alone is also capable of capturing Apo E and binding to the LDL receptor (Vinagre et al., 2007), indicating that the incorporated drugs should have little influence on the external part of the particle.

4. SAXS

Experimental data of SAXS for LDE (green), LDE-PTX (purple), LDE-MTX (orange), and LDE-ETO (blue) samples are presented in Fig. 7. Unlike USAXS measurements, SAXS data were performed to obtain information from inside the nanoparticles. The *p(r)* presented in Fig. 7B

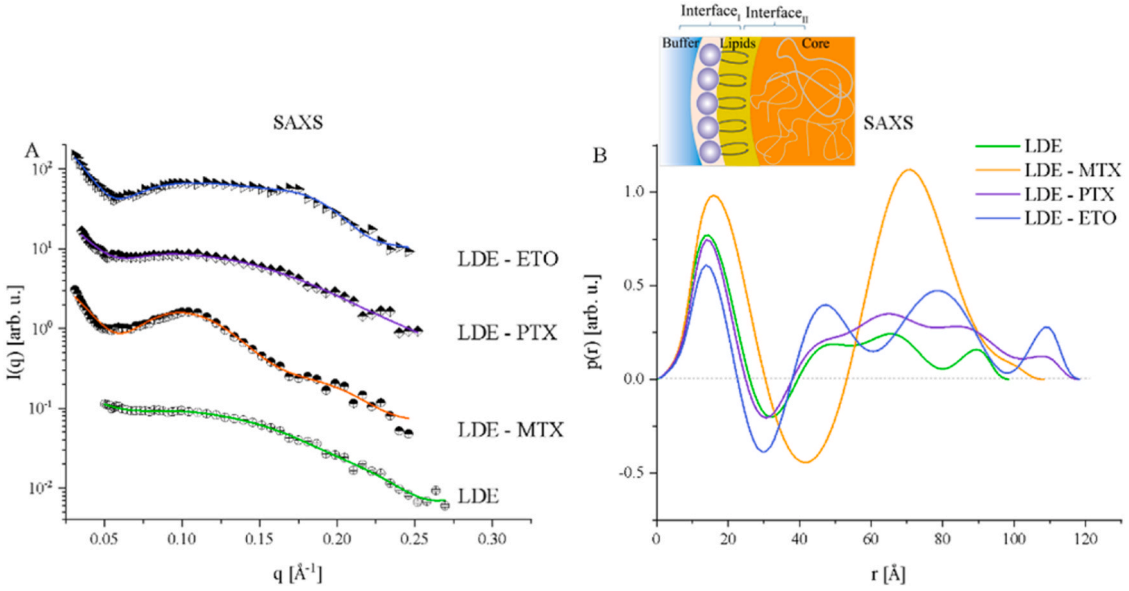

Fig. 7. IFT applied to LDE and LDE-associations SAXS data. A) Fitting (linear curve) of scattering data (circles) of samples by the IFT method. B) Pair distance distribution functions, p(r), obtained from the decoupling procedure with IFT method for all samples. The insert in Fig. 7B informs about the region of p(r) corresponding to the regions inside the particle.

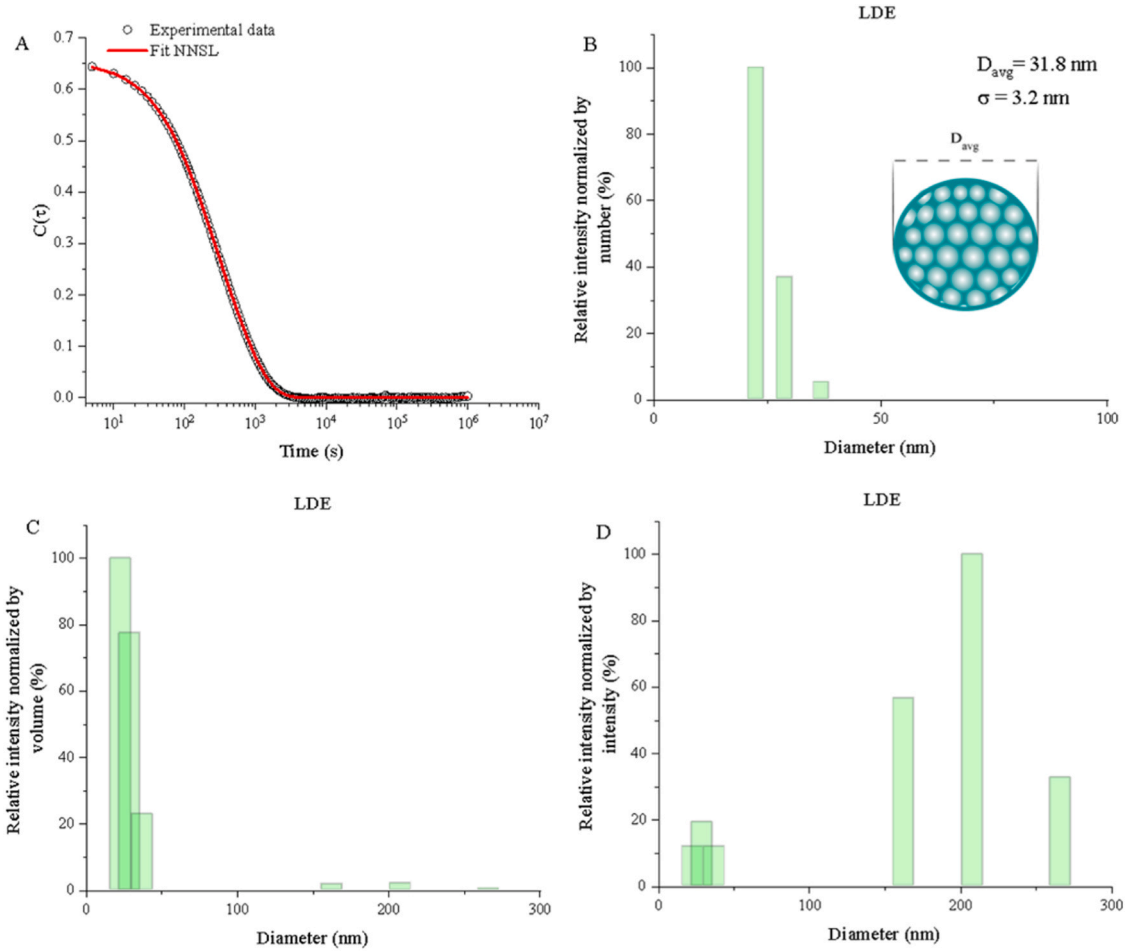

Fig. 8. DLS results for LDE samples. A) DLS experimental autocorrelation curves. B) Diameter distribution by relative intensity normalized number. C)Diameter distribution by relative intensity normalized volume. D)Diameter distribution by relative intensity normalized intensity.

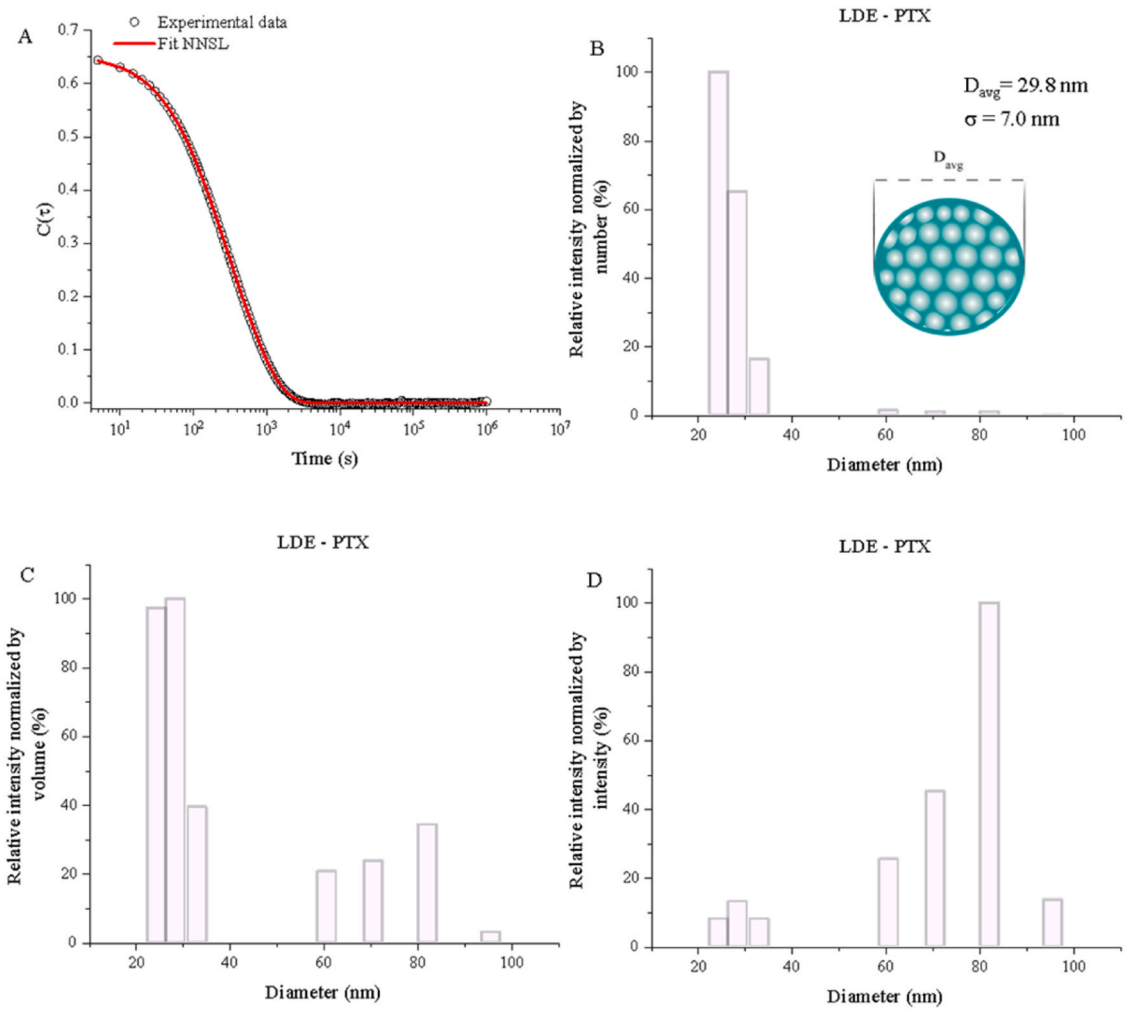

Fig. 9. DLS results for LDE-PTX samples. A) DLS experimental autocorrelation curves. B) Diameter distribution by relative intensity normalized number. C)Diameter distribution by relative intensity normalized volume. D)Diameter distribution by relative intensity normalized intensity.

indicate a core-shell structure, i.e., with different electronic densities. In the shell region (lipid heads) we have positive values in the *p(r)*, followed by negative values in the core region (lipid shells and cholesterol esters) This behavior is observed in all investigated samples. The undulations in *p(r)*, starting at 50 Å, are related to cholesterol esters and/or associated drugs (within the nanoparticle), that may have different encapsulation configurations. Due to the low resolution of the SAXS technique, it is not possible to establish the thickness of the shell and the maximum diameter of the core. However, LDE-MTX *I(q)* present a more pronounced undulation pattern, when compared with the other samples. This can be an indicative that MTX is forming a layer inside the core. In all the cases, LDE and LDE-associations, *I(q)* indicate that there is some degree of organization inside the core.

Due to the low resolution of the SAXS technique, we can analyze the patterns of I(q) for the samples and the p(r) calculated by IFT, as the presence of interfaces in terms of electronic density contrasts. Analyzing the *I(q)* curves, we can see that LDE-ETO show a weak peak at q=0.17 $Å^{-1}$, corresponding to a repeating distance of ~ 4 nm (see Supplemental Material). This may indicate a periodic organization of the ETO in the core of the LDE particle. Scherrer equation (26) was used to estimate the size of a crystallite (D) from the width of the peak observed in *I(q)*. We obtained that LDE-ETO has a crystallite size of D = 8.4 nm. The LDE-MTX association presents a more pronounced peak at 0.11 $Å^{-1}$, corresponding to a repeating distance of 5.7 nm. LDE-MTX has a crystallite size of D = 2.5 nm. This may indicate a periodic organization of the MTX in the core of the LDE particle. In the LDE and LDE-PTX scattering curves it was not possible to clearly identify peaks, indicating a more homogeneous distribution of the molecules in the particle core.

Each side of the interfaces has a different electron density compared to the buffer (water), as schematized in the insert of Fig. 7B. Our results of SAXS indicate that the drug is mainly incorporated in the core of the LDE.

5. DLS

DLS experimental results are presented in Figs. 8–11. The hydrodynamic radius analysis was performed using the Non-Negative Least Squares (NNLS) method for multimodal systems, with heterogeneous particle size distributions.

Fig.8A shows the autocorrelation function $g^{(1)}(\tau)$ of LDE sample. Fig.8B-D present the diameter values corresponding to the mean size found in number, volume and intensity normalization distributions obtained using NNLS algorithm. DLS relative intensity normalized by number results indicate that samples, under these conditions, have some polydispersity (σ = 3.2 nm) in solution. Although it is possible to observe that DLS relative intensity normalized by intensity and volume present contribution from large particles (aggregates) in solution, however, in number, this aggregate contribution is not significant.

In Fig.8 C-D we observe contributions, normalized by volume and intensity respectively, of large particles (150–275 nm). However, we know that LDE in solution at room temperature can form aggregates, which in turn will contribute to the DLS scattering and therefore

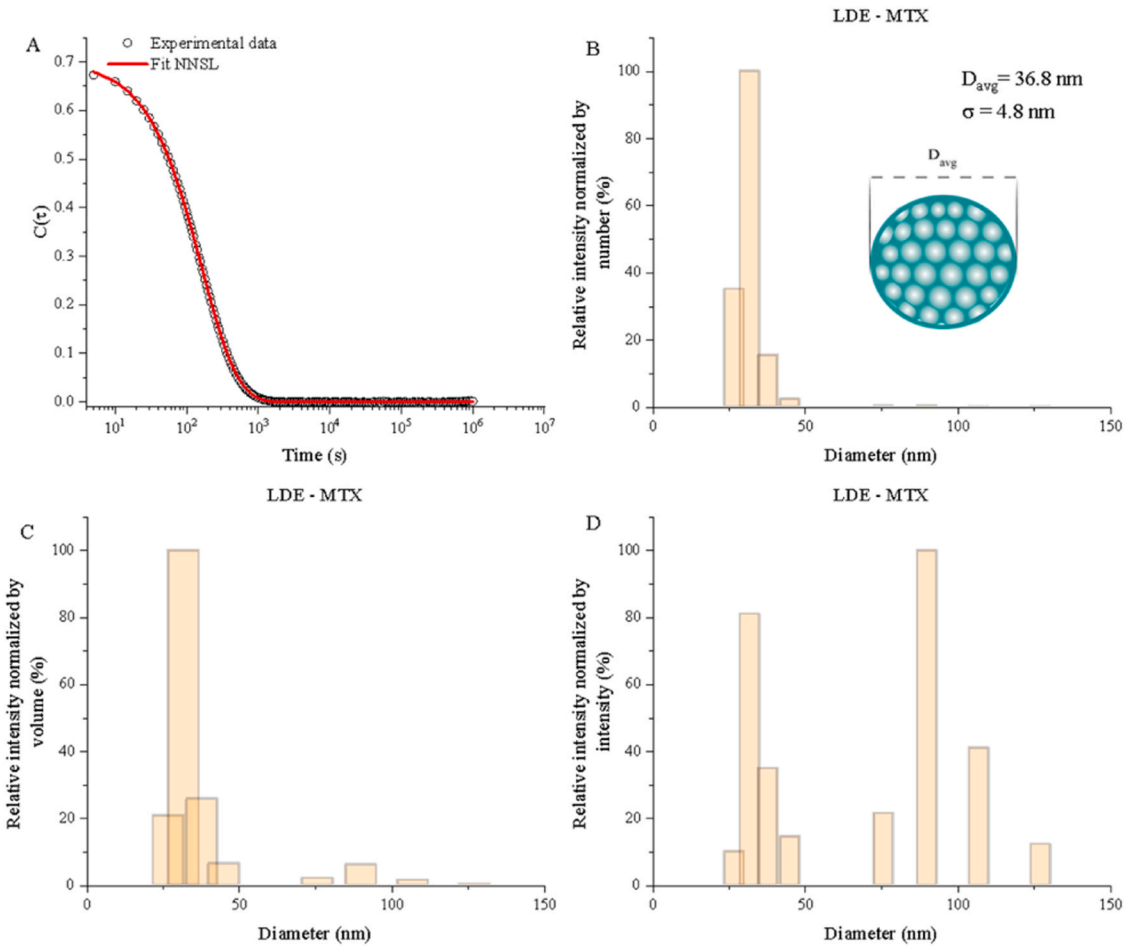

Fig. 10. DLS results for LDE-MTX samples. A) DLS experimental autocorrelation curves. B) Diameter distribution by relative intensity normalized number. C) Diameter distribution by relative intensity normalized volume. D)Diameter distribution by relative intensity normalized intensity.

contributions in volume and intensity are observed. However, when we compare the data normalized by number (Fig. 8 B) the contribution is negligible, so that most particles have an average size of approximately 32 nm.

Fig. 9A shows the autocorrelation function $g^{(1)}(\tau)$ of LDE-PTX sample. Fig. 9B-D present the diameter values corresponding to the mean size found in number, volume and intensity normalization distributions obtained using NNLS algorithm. DLS relative intensity normalized by number results indicate that samples, under these conditions, have some polydispersity (σ = 7.0 nm) in solution. Although it is possible to observe that DLS relative intensity normalized by intensity and volume present contribution from aggregates in solution, however, in number, this aggregate contribution is not significant. It can indicate that even in low concentration LDE-PTX sample, can form particle aggregation.

In Fig. 9C-D we observe contributions, normalized by volume and intensity respectively, of large particles (60–90 nm). However, we know that LDE-PTX in solution at room temperature can form aggregates, which in turn will contribute to the DLS scattering and therefore contributions in volume and intensity are observed. However, when we compare the data normalized by number (Fig. 9B) the contribution is negligible, so that most particles have an average size of approximately 30 nm.

Fig. 10A shows the autocorrelation function $g^{(1)}(\tau)$ of LDE-MTX sample. Fig. 10B-D present the diameter values corresponding to the mean size found in number, volume and intensity normalization distributions obtained using NNLS algorithm. DLS relative intensity normalized by number results indicate that samples, under these conditions, have some polydispersity (σ = 4.8 nm) in solution. Although it is possible to observe that DLS relative intensity normalized by intensity and volume present contribution from aggregates in solution, however, in number, this aggregate contribution is not significant.

In Fig. 10C-D we observe diameter distribution normalized by volume and intensity respectively, of large particles (75–125 nm). However, we know that LDE-MTX in solution at room temperature can form aggregates, which in turn will contribute to the DLS scattering and therefore contributions in volume and intensity are observed. However, when we compare the data normalized by number (Fig. 10B) the contribution is negligible, so that most particles have an average size of approximately 37 nm.

Fig. 11A shows the autocorrelation function $g^{(1)}(\tau)$ of LDE-ETO sample. Fig. 11B-D present the diameter values corresponding to the mean size found in number, volume and intensity normalization distributions obtained using NNLS algorithm. DLS relative intensity normalized by number results indicate that samples, under these conditions, have low polydispersity (σ = 3.6 nm) in solution. Although it is possible to observe that DLS relative intensity normalized by intensity and volume present contribution from aggregates in solution, however, in number, this aggregate contribution is not significant.

In Fig. 11C-D we observe contributions, normalized by volume and intensity respectively, of large particles (90–140 nm). However, we know that LDE-ETO in solution at room temperature can form aggregates, which in turn will contribute to the DLS scattering and therefore contributions in volume and intensity are observed. However, when we compare the data normalized by number (Fig. 11B) the contribution is negligible, so that most particles have an average size of approximately 34 nm.

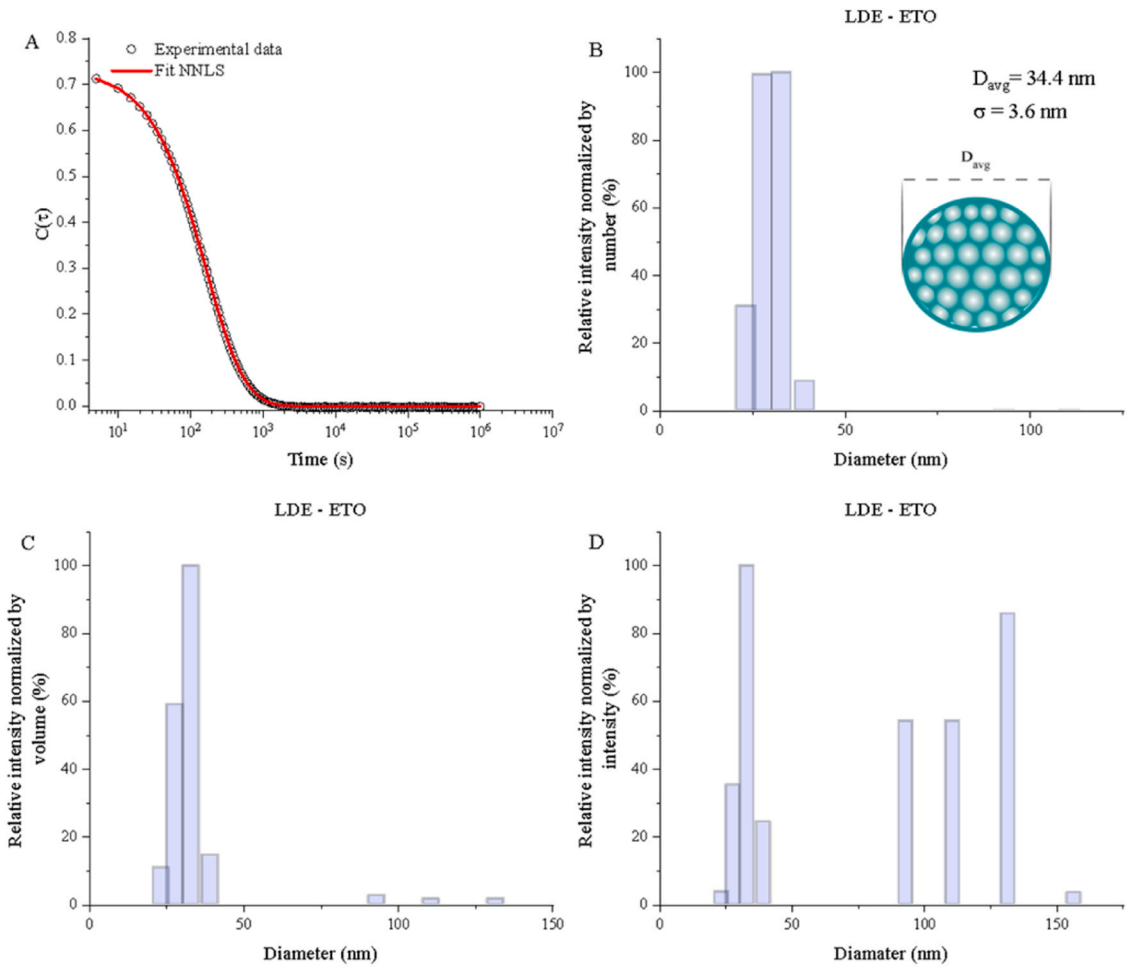

Fig. 11. DLS results for LDE-ETO samples. A) DLS experimental autocorrelation curves. B) Diameter distribution by relative intensity normalized number. C) Diameter distribution by relative intensity normalized volume. D) Diameter distribution by relative intensity normalized intensity.

Table 1
Diameters obtained by USAXS and DLS. And comparison with typical values (nm) found in the literature. The number in parentheses indicates the reference.

Techniques	LDE	LDE-PTX	LDE-MTX	LDE-ETO
DLS $_{number}$ (nm)	31.2 ± 3.2	29.8 ± 7.0	36.8 ± 4.8	34.4 ± 3.6
USAXS (nm)	32.5 ± 2.8	32.0 ± 3.5	34.5 ± 2.2	37.5 ± 2.5
Refs. – DLS (nm)	40 (Maranhao et al., 2011)	85 ± 10 (Pires et al., 2009)	60 (Maranhao et al., 2011)	65 ± 10 (Prete et al., 2010)
DLS $_{intensity}$ (nm)	45.1 ± 2.4	78.1 ± 2.2	57.9 ± 4.0	63.4 ± 3.0

When our diameter values are compared with those typically found in the literature, indicated in Table 1, an incompatibility in diameters is observed. This can be explained by the analysis carried out by the studies indicated (in Table 1), where the average diameters were obtained with respect to the scattering intensity (DLS) and not by the NNLS method, which analyzes the relative intensity by number, as done in the present work. Data in the literature are different from those obtained here, due to the analysis method. If we calculate the diameter normalized by intensity, we would obtain values close to those in the literature. The light scattering intensity, in DLS technique, depends on the sixth power of the particle diameter (Aragón and Pecora, 1976). Therefore, the larger the particle, the greater the contribution. However, the number of large particles in our study is very small. Therefore, considering the DLS results, normalized by intensity, is not the best way to describe the particle size distribution. Consequently, larger particles contribute to the total scattering intensity exponentially more with increasing size, making DLS particularly sensitive for clustering compared to smaller particles.

It is important to highlight that, differently from the USAXS, SAXS data did not allow the calculation of the average size of the particles in solution. The size distribution of LDE-associations determined in our work (~ 35 nm) is essential for the effectiveness of the drug action in the cells. It is known that large particles (~ 70 nm) are less effective in the drug treatment (Freitas et al., 2018). It is well known that LDL have a size distribution between 25 and 30 nm (Ambrosch et al., 1998; Vekic et al., 2022), so it is important that the LDE nanoemulsion is compatible with this size distribution.

To investigate the stability of the size distribution by DLS, we performed measurements over seven consecutive days under the same experimental conditions described in material and methods. Fig. 12 shows the reproducibility of DLS data over 7 days of measurements under the same conditions. The small variations observed for diameter (nm) over the days are within the error of each measurement.

Over time, LDE and LDE-associated drugs proved to be stable from the point of view of size distribution. This is essential for this preparation to be effective in combating cancer.

6. Conclusions

This study shows that the size distribution of the LDE nanoparticles alone or associated with chemotherapeutic agents have reproducible

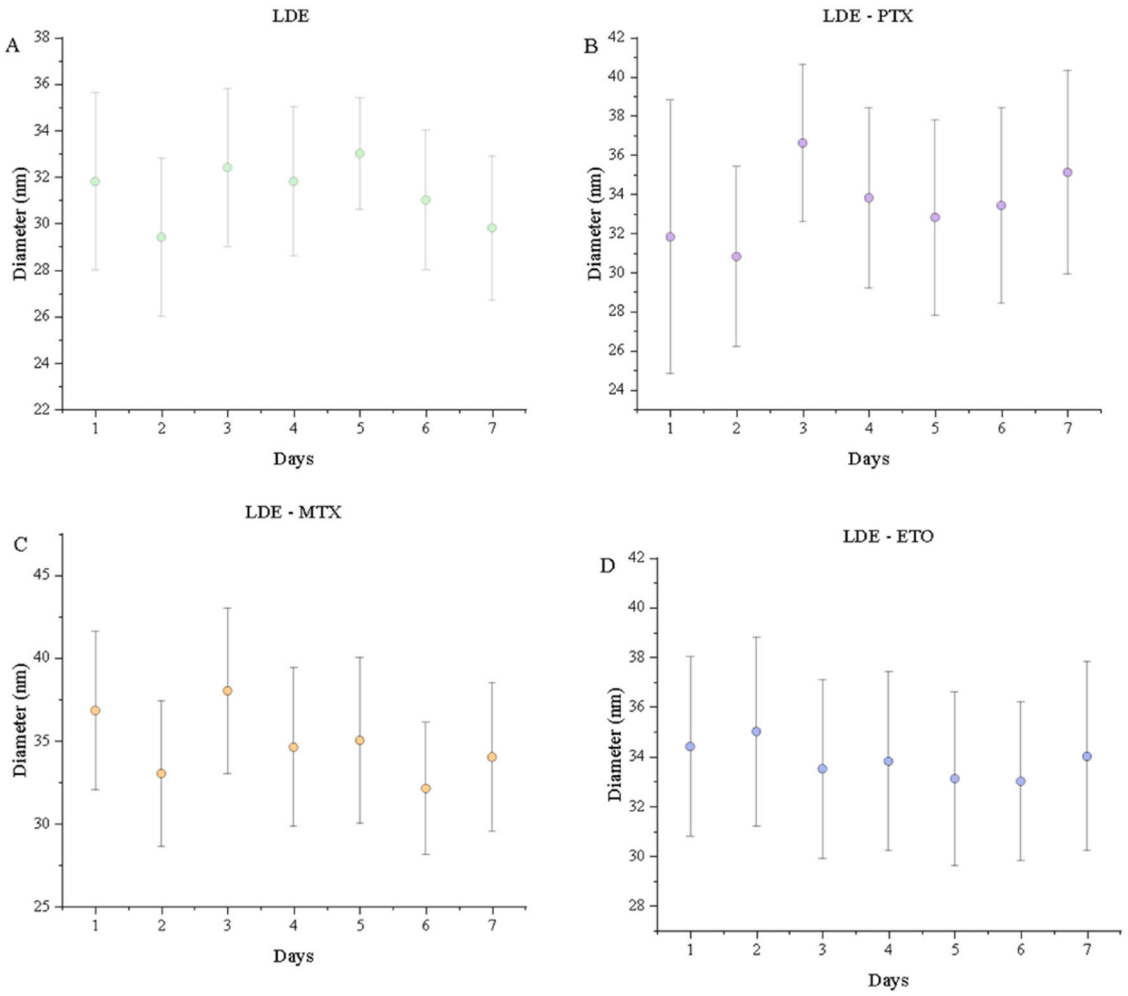

Fig. 12. DLS measurements were carried out on consecutive days to analyze the reproducibility of the results obtained. A) Diameter vs. Days to LDE. B) Diameter vs. Days for LDE – PTX. C) Diameter vs. Days for LDE – MTX. D) Diameter vs. Days for LDE – ETO.

and stable values for 3 months, as indicated by both DLS and USAXS techniques. The maximum diameter of LDE documented in this study by DLS, which is larger than that reported in previous studies, which can be accounted for and in fact are complementary to each other since they represent different DLS measurement perspectives. The current SAXS results show that inside the nanoparticles where the MTX and ETO were incorporated, a periodicity was observed. Furthermore, cholesterol esters and the associated drugs, located in the nanoparticle core, seem to have different encapsulation configurations. LDE formulations with associated PTX, ETO or MTX were previously tested in animal experiments and subsequent in small clinical trials enrolling patients with solid and hematologic cancers or with cardiovascular disease. Promising results were obtained with all three preparations regarding low toxicity, optimal tolerability and possibly superior pharmacological action. Thus, by strengthening the knowledge of the structural aspects of those LDE preparations, our results may contribute to potentially important therapeutic developments in Nanomedicine.

Funding sources

This study was supported by the National Council for Scientific and Technological Development [grant number 465259/2014-6]; Coordination for the Improvement of Higher Education Personnel (CAPES); National Institute of Science and Technology Complex Fluids (INCT-FCx) [grant number 370832/2023-0], and FAPESP [grant numbers 2014/50983-3, 2016/24531-3 and 2020/1625].

Declaration of Competing Interest

The authors declare that they have no known competing financial interests or personal relationships that could have appeared to influence the work reported in this article.

Data Availability

Data will be made available on request.

Acknowledgements

The authors are thankful Gabriel Teobaldo, Dennys Reis, Débora Fernandes and Wanderley Gomes were helpful in the experiments and Dr. Cristiano L.P. de Oliveira contributed to the analysis of the X-ray scattering data.

Appendix A. Supporting information

Supplementary data associated with this article can be found in the online version at doi:10.1016/j.chemphyslip.2024.105418.

References

Ahmed, A.A., Dash, S., 2017. Application of novel nanoemulsion in drug targeting. Res. J. Pharm. Technol. Vol. 10.

Alanazi, F.K., Haq, N., Radwan, A.A., Alsarra, I.A., Shakeel, F., 2015. Formulation and evaluation of cholesterol-rich nanoemulsion (LDE) for drug delivery potential of cholesteryl-maleoyl-5-fluorouracil. Pharm. Dev. Technol. 20 (3).
Ambrosch, A., Mühlen, I., Kopf, D., Augustin, W., Dierkes, J., König, W., et al., 1998. LDL size distribution in relation to insulin sensitivity and lipoprotein pattern in young and healthy subjects. Diabetes Care 21 (12).
Aragón, S.R., Pecora, R., 1976. Theory of dynamic light scattering from polydisperse systems. J. Chem. Phys. 64 (6).
Dias, M.L.N., Carvalho, J.P., Rodrigues, D.G., Graziani, S.R., Maranhão, R.C., 2007. Pharmacokinetics and tumor uptake of a derivatized form of paclitaxel associated to a cholesterol-rich nanoemulsion (LDE) in patients with gynecologic cancers. Cancer Chemother. Pharm. 59 (1).
Freitas, S.C.M.P., Tavares, E.R., Silva, B.M.O., Meneghini, B.C., Kalil-Filho, R., Maranhão, R.C., 2018. Lipid core nanoparticles resembling low-density lipoprotein and regression of atherosclerotic lesions: effects of particle size. Braz. J. Med Biol. Res 51 (3).
Glatter, O., 1977. A new method for the evaluation of small-angle scattering data. J. Appl. Crystallogr 10 (5).
Greenwood, A.I., Tristram-Nagle, S., Nagle, J.F., 2006. Partial molecular volumes of lipids and cholesterol. Chem. Phys. Lipids 143, 1–2.
Koppel, D.E., 1972. Analysis of macromolecular polydispersity in intensity correlation spectroscopy: the method of cumulants. J. Chem. Phys. 57 (11).
Mahato, R., 2017. Nanoemulsion as targeted drug delivery system for cancer therapeutics. J. Pharm. Sci. Pharm. 3 (2).
Maranhao, R., Moura, J., Valduga, Tavares, Maranhao, R., Maria, 2011. Novel formulation of a methotrexate derivative with a lipid nanoemulsion. Int J. Nanomed.
Maranhão, R.C., Cesar, T.B., Pedroso-Mariani, S.R., Hirata, M.H., Mesquita, C.H., 1993. Metabolic behavior in rats of a nonprotein microemulsion resembling low-density lipoprotein. Lipids 28 (8).
Maranhão, R.C., Garicochea, B., Silva, E.L., Dorlhiac-Llacer, P., Cadena, S.M.S., Coelho, I. J.C., et al., 1994. Plasma kinetics and biodistribution of a lipid emulsion resembling low-density lipoprotein in patients with acute leukemia. Cancer Res 54 (17).
Mello, S.B.V., Tavares, E.R., Bulgarelli, A., Bonfá, E., Maranhão, R.C., 2013. Intra-articular methotrexate associated to lipid nanoemulsions: Anti-inflammatory effect upon antigen-induced arthritis. Int J. Nanomed. 8.
Montis, C., Zendrini, A., Valle, F., Busatto, S., Paolini, L., Radeghieri, A., et al., 2017. Size distribution of extracellular vesicles by optical correlation techniques. Colloids Surf. B Biointerfaces 158.
Occhiutto, M.L., Maranhão, R.C., Costa, V.P., Konstas, A.G., 2020. Nanotechnology for medical and surgical glaucoma therapy—a review. Adv. Ther. Vol. 37.
Oliveira, C.L.P., Behrens, M.A., Pedersen, J.S., Erlacher, K., Otzen, D., Pedersen, J.S., 2009. A SAXS study of glucagon fibrillation. J. Mol. Biol. 387 (1).
Pedersen, J.S., Hansen, S., Bauer, R., 1994. The aggregation behavior of zinc-free insulin studied by small-angle neutron scattering. Eur. Biophys. J. 22 (6).
Pepineli, R., Santana, A.C., Silva, F.M.O., Tavoni, T.M., Stolf, N.A.G., Noronha, I.L., et al., 2021. Use of paclitaxel carried in lipid nanoparticles to treat aortic allograft transplantation in rats. J. Pharm. Pharm. 73 (8).
Pinheiro, K.V., Hungria, V.T.M., Ficker, E.S., Valduga, C.J., Mesquita, C.H., Maranhão, R. C., 2006. Plasma kinetics of a cholesterol-rich microemulsion (LDE) in patients with Hodgkin's and non-Hodgkin's lymphoma and a preliminary study on the toxicity of etoposide associated with LDE. Cancer Chemother. Pharm. 57 (5).
Pires, L.A., Hegg, R., Valduga, C.J., Graziani, S.R., Rodrigues, D.G., Maranhão, R.C., 2009. Use of cholesterol-rich nanoparticles that bind to lipoprotein receptors as a vehicle to paclitaxel in the treatment of breast cancer: pharmacokinetics, tumor uptake and a pilot clinical study. Cancer Chemother. Pharm. 63 (2).
Prete, A.C.Lo, Maria, D.A., Rodrigues, D. bora G., Valduga, C.J., Ibañez, O.C.M., Maranhão, R.C., 2010. Evaluation in melanoma-bearing mice of an etoposide derivative associated to a cholesterol-rich nanoemulsion. J. Pharm. Pharm. 58 (6).
Priya, S., Desai, V.M., Singhvi, G., 2022. Surface Modification of lipid-based nanocarriers: a potential approach to enhance targeted drug delivery. ACS Omega.
Schneider, H., Morrod, R.S., Colvin, J.R., Tattrie, N.H., 1973. The lipid core model of lipoproteins. Chem. Phys. Lipids 10 (4).
Teixeira, R.S., Curi, R., Maranhão, R.C., 2010. Effects on Walker 256 tumour of carmustine associated with a cholesterol-rich microemulsion (LDE). J. Pharm. Pharm. 56 (7).
Valduga, C.J., Fernandes, D.C., Prete, A.C.Lo, Azevedo, C.H.M., Rodrigues, D.G., Maranhão, R.C., 2010. Use of a cholesterol-rich microemulsion that binds to low-density lipoprotein receptors as vehicle for etoposide. J. Pharm. Pharm. 55 (12).
Vekic, J., Zeljkovic, A., Cicero, A.F.G., Janez, A., Stoian, A.P., Sonmez, A., et al., 2022. Atherosclerosis development and progression: the role of atherogenic small, dense LDL. Medicines 58 (2).
Vinagre, C.G.C., Ficker, E.S., Finazzo, C., Alves, M.J.N., De Angelis, K., Irigoyen, M.C., et al., 2007. Enhanced removal from the plasma of LDL-like nanoemulsion cholesteryl ester in trained men compared with sedentary healthy men. J. Appl. Physiol. 103 (4).